A Finite-Element / Boundary-Element Method for the Simulation of Coupled Electrostatic-Mechanical Systems

M. Kaltenbacher, H. Landes, R. Lerch, F. Lindinger

▶ **To cite this version:**

M. Kaltenbacher, H. Landes, R. Lerch, F. Lindinger. A Finite-Element / Boundary-Element Method for the Simulation of Coupled Electrostatic-Mechanical Systems. Journal de Physique III, 1997, 7 (10), pp.1975-1982. 10.1051/jp3:1997236 . jpa-00249695

HAL Id: jpa-00249695
https://hal.science/jpa-00249695

Submitted on 4 Feb 2008

HAL is a multi-disciplinary open access archive for the deposit and dissemination of scientific research documents, whether they are published or not. The documents may come from teaching and research institutions in France or abroad, or from public or private research centers.

L'archive ouverte pluridisciplinaire **HAL**, est destinée au dépôt et à la diffusion de documents scientifiques de niveau recherche, publiés ou non, émanant des établissements d'enseignement et de recherche français ou étrangers, des laboratoires publics ou privés.

A Finite-Element / Boundary-Element Method for the Simulation of Coupled Electrostatic-Mechanical Systems (*)

M. Kaltenbacher (**), H. Landes, R. Lerch and F. Lindinger

Department of Electrical Measurement Technology, University of Linz Altenbergerstr. 69, 4040 Linz, Austria

(Received 20 March 1996, revised 11 June 1997, accepted 7 july 1997)

PACS 41.20.Cv – Electrostatics, Poisson and Laplace equations, boundary-value problems
PACS.02.70.Dh – Finite-element and Galerkin methods
PACS.02.70 Pt – Boundary-integral methods

Abstract. — A recently developed modeling scheme for the numerical simulation of coupled electrostatic-mechanical systems such as electrostatic transducers is presented. The scheme allows the calculation of dynamic rigid motions as well as deformations of materials in an electric field. The coupled system, described by the equations governing the electric and mechanical field, is solved by a combined Finite-Element/Boundary-Element-Method (FEM-BEM) Computer simulations of a micropump and of an acceleration sensor are presented demonstrating the efficiency of the developed algorithm.

1. Introduction

In electrostatic-mechanical systems a material is subject both to rigid motions and to elastic deformations, which in turn may strongly influence the electric field and thus the electric force distribution A typical electrostatic-mechanical system is a micromachined pump [1], shown in Figure 1. If an electric voltage is applied to the electrodes, the elastic pump diaphragm (electrode 2) is deformed by the electrostatic force and bends towards the counterelectrode (electrode 1). Thereby, fluid will be sucked in through the inlet valve. When the supply voltage is switched off, the relaxation of the diaphragm will push the fluid through the outlet valve.

2. Governing Equations

The electric field in a region containing no free electric charges can be described by

$$\nabla \cdot \varepsilon \nabla \phi = 0 \tag{1}$$

Here, ε denotes the permittivity tensor and ϕ the scalar electric potential.

(*) This paper was presented at NUMELEC'97
(**) Author for correspondence (e-mail: m.kaltenbacher@jk.uni-linz ac.at)

© Les Éditions de Physique 1997

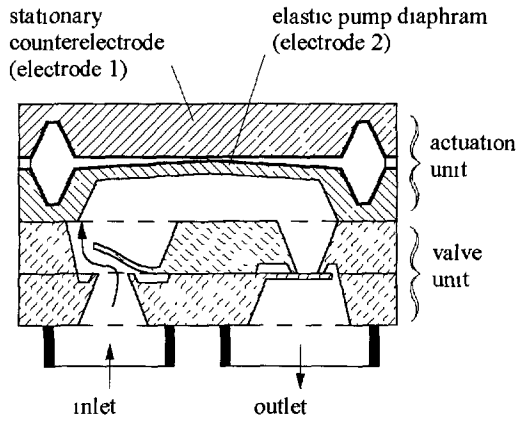

Fig. 1. — Schematic view of an electrostatically driven micropump [1].

In the case of linear elasticity and isotropic materials, the dynamic behaviour of mechanical systems can be described by

$$\frac{E}{2(1+\nu)}\left((\nabla\cdot\nabla)\mathbf{d}+\frac{1}{1-2\nu}\nabla(\nabla\cdot\mathbf{d})\right)+\mathbf{f}=\rho\frac{\partial^2\mathbf{d}}{\partial t^2} \tag{2}$$

where $\mathbf{d}$ is the mechanical displacement, $\mathbf{f}$ the applied mechanical force, E the modulus of elasticity, ν Poisson's ratio and ρ the density.

The electrostatic force between the electrodes is calculated based on the electrostatic force tensor T_E, where $\mathbf{E}=(E_x,\ E_y,\ E_z)$ denotes the electric field

$$T_E=\begin{bmatrix} \varepsilon E_x^2-\frac{1}{2}\varepsilon|\mathbf{E}|^2 & \varepsilon E_xE_y & \varepsilon E_xE_z \\ \varepsilon E_yE_x & \varepsilon E_y^2-\frac{1}{2}\varepsilon|\mathbf{E}|^2 & \varepsilon E_yE_z \\ \varepsilon E_zE_x & \varepsilon E_zE_y & \varepsilon E_z^2-\frac{1}{2}\varepsilon|\mathbf{E}|^2 \end{bmatrix}. \tag{3}$$

The electrostatic force $\mathbf{F}_E$ is given by

$$\mathbf{F}_E=\int\!\!\int_A T_E\mathbf{n}\,\mathrm{d}S, \tag{4}$$

where $\mathbf{n}$ is the normal vector.

3. FEM-BEM-Coupling

The boundary element discretization of (1) yields the following BE-matrix equation

$$H_\phi\ \{\Phi\}=G_\phi\{\Phi_n\} \tag{5}$$

with the two boundary element matrices H_ϕ and G_ϕ, the nodal vector $\{\Phi\}$ of the scalar electric potential and the nodal vector $\{\Phi_n\}$ of the normal derivatives of the scalar electric potential.

Applying the FE-formulation to (2) leads to the well-known matrix equation for the mechanical quantities

$$M\{\ddot{d}\}+C\{\dot{d}\}+K\{d\}-\{F(\Phi,\Phi_n)\}=\{0\} \tag{6}$$

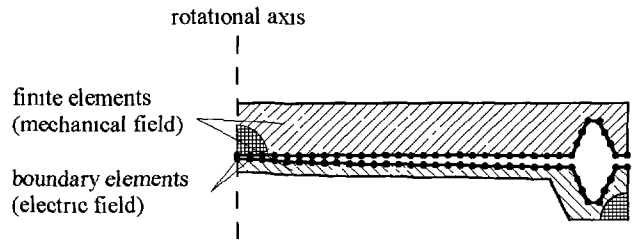

Fig. 2. — FEM/BEM discretization of the actuation unit (Fig. [1]).

with mass matrix M, damping matrix C, stiffness matrix K, force vector $\{F\}$ including the nonlinear term, nodal accelerations $\{\ddot{d}\}$, nodal velocities $\{\dot{d}\}$ and nodal displacements $\{d\}$.

The FEM/BEM discretization of the actuation unit (Fig. 1) is performed according to Figure 2. Finite elements are used to describe the mechanical field in the two electrodes, whereas the electric field in the gap between is modeled by boundary elements. This approach has the advantage, that the elastic pump diaphragm (electrode 2) can move towards the stationary counterelectrode (electrode 1) without deforming any finite elements which would otherwise (with pure FE-modeling) be necessary to describe the electric field.

The two boundary element matrices H_ϕ and G_ϕ have to be updated corresponding to the mechanical displacement.

4. Calculation Scheme

The use of the *Newmark Method* [2] with the two integration parameters β and γ_H for the time discretization of (6), leads to the following predictor/corrector algorithm:

Predictor:

$$\{\tilde{d}\} = \{d\}^n + \Delta t\{v\}^n + \frac{1}{2}\Delta t^2(1-2\beta)\{a\}^n \tag{7}$$

$$\{\tilde{v}\} = \{v\}^n + (1-\gamma_H)\Delta t\{a\}^n \tag{8}$$

Equation:

$$M^*\{a\}^{n+1} = \{F(\{\Phi\}^{n+1}, \{\Phi_n\}^{n+1})\} - K\{\tilde{d}\} - C\{\tilde{v}\}$$

$$M^* = M + \gamma_H \Delta t C + \beta \Delta t^2 K \tag{9}$$

Corrector:

$$\{d\}^{n+1} = \{\tilde{d}\} + \beta\Delta t^2\{a\}^{n+1} \tag{10}$$

$$\{v\}^{n+1} = \{\tilde{v}\} + \gamma_H\Delta t\{a\}^{n+1} \tag{11}$$

The direct coupling of (5) and (6) leads to a nonlinear system of equations. Using predictor values for the calculation of the electrostatic force, a decoupling into an electrical and mechanical matrix equation can be achieved. To ensure the strong coupling between the electrical and mechanical quantities the following Predictor/Multicorrector Algorithm similar to [3] is used·

STEP 1: Set the iteration counter i to zero and define the predictor values as follows:

Electrical quantities:

$$^i\{\tilde{\Phi}\} = \{\Phi\}^n \tag{12}$$

$$^i\{\tilde{\Phi}_n\} = \{\Phi_n\}^n \tag{13}$$

Mechanical quantities:

$$^{i}\{\tilde{d}\} = \{d\}^{n} + \Delta t\{v\}^{n} + \frac{1}{2}(1-2\beta)\Delta t^{2}\{a\}^{n} \quad (14)$$

$$^{i}\{\tilde{v}\} = \{v\}^{n} + (1-\gamma_{H})\Delta t\{a\}^{n} \quad (15)$$

$$\{\tilde{a}\} = \{0\} \quad (16)$$

STEP 2: Solve matrix equation system for the electrical and mechanical quantities:

$$\begin{pmatrix} H_{\phi} & -G_{\phi} & 0 \\ 0 & 0 & M^{*} \end{pmatrix} \begin{pmatrix} \{\Delta\Phi\} \\ \{\Delta\Phi_{n}\} \\ \{\Delta a\} \end{pmatrix} = \begin{pmatrix} \{\Delta Q_{1}\} \\ \{\Delta Q_{2}\} \end{pmatrix} \quad (17)$$

$$\{\Delta Q_{1}\} = -H_{\phi}\,^{i}\{\tilde{\Phi}\} + G_{\phi}\,^{i}\{\tilde{\Phi}_{n}\} \quad (18)$$

$$\{\Delta Q_{2}\} = \{F(^{i}\{\tilde{\Phi}\}, ^{i}\{\tilde{\Phi}_{n}\})\} - K\{\tilde{d}\} - C\{\tilde{v}\} - M\{\tilde{a}\} \quad (19)$$

STEP 3: Perform the corrector phase (predictor update).
Electrical quantities.

$$^{i+1}\{\tilde{\Phi}\} = ^{i}\{\tilde{\Phi}\} + \{\Delta\Phi\} \quad (20)$$

$$^{i+1}\{\tilde{\Phi}_{n}\} = ^{i}\{\tilde{\Phi}_{n}\} + \{\Delta\Phi_{n}\} \quad (21)$$

Mechanical quantities:

$$^{i+1}\{\tilde{d}\} = ^{i}\{\tilde{d}\} + \beta\Delta t^{2}\{\Delta a\} \quad (22)$$

$$^{i+1}\{\tilde{v}\} = ^{i}\{\tilde{v}\} + \gamma_{H}\Delta t\{\Delta a\} \quad (23)$$

$$^{i+1}\{\tilde{a}\} = ^{i}\{\tilde{a}\} + \{\Delta a\} \quad (24)$$

STEP 4: Next iteration: go to STEP 2.
STEP 5. Solution for time step $(n+1)$.

In (12)−(24), i denotes the iteration counter, $\{\Delta Q_1\}$ and $\{\Delta Q_2\}$ the residual vectors of the right hand side for iteration i and $\{\Delta a\}$, $\{\Delta\Phi\}$ and $\{\Delta\Phi_n\}$ the solution vectors of the current iteration. The main difference from a standard iteration algorithm lies in the fact, that the right hand side vectors of iteration i are calculated from the difference of the source vectors and the solution of iteration i As a result, the residual of the right hand side vectors as well as the solution vectors converge to zero by increasing iteration and, can be used for stopping the iteration. According to the mechanical displacement the boundary matrices G and H have to be updated. For linear elasticity the matrices M, C and K remain constant throughout the whole simulation. For a time step value Δt, considering the physical behaviour of the structure, no more than 2 iterations were necessary. Iterative solvers - GMRES (Generalized Minimum Residual) and CGS (Conjugate Gradient Squared) - have been adapted to solve (17) in a very fast way. The flow chart describing the algorithm is shown in Figure 3.

5. Verification

The verification of the calculation scheme described above has been performed by computing several analytically computable problems. In one of these examples the deformations of two circular plates due to an applied electric voltage have been calculated. Figure 4 shows the relative error of the calculated deformations compared to the analytical solution for two different boundary conditions. The clamped plate experiences a greater bending moment than the simply supported one. The use of linear interpolation functions in the finite element scheme, results in a greater relative error (Fig. 4).

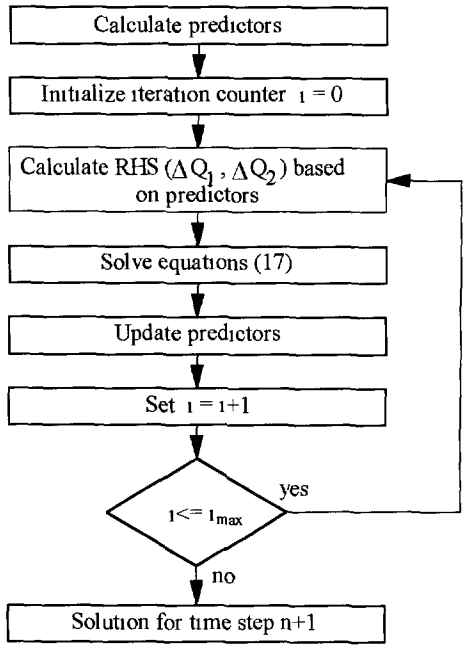

Fig. 3. — Calculation scheme.

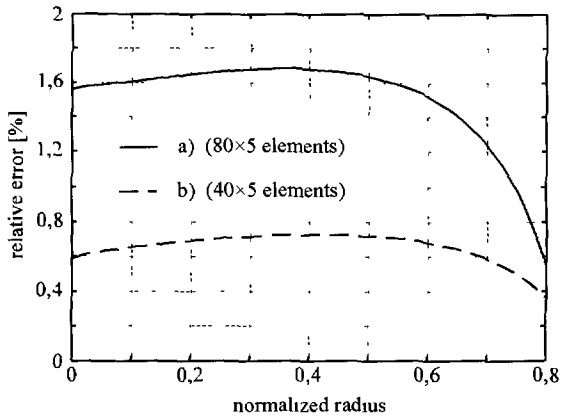

Fig. 4 — Relative error of numerically calculated displacements compared to analytical solution for two different boundary conditions a) Clamped plate. b) Simply supported plate.

6. Applications

6.1. MICROPUMP. — In a first example, the micromachined pump, as already shown in Figure 1, was modeled. This pump has a diameter of 7 mm, a total height of about 1 mm and a gap thickness of 4 μm between the elastic pump diaphragm and the counterelectrode. Figure 5 shows the mechanical deformations of the actuation unit when a dc voltage is applied. One point of investigation was the nonlinear dynamic response of the micropump. The pump was excited by a sinusoidal voltage with a frequency of 1 kHz and different amplitudes. The dynamic

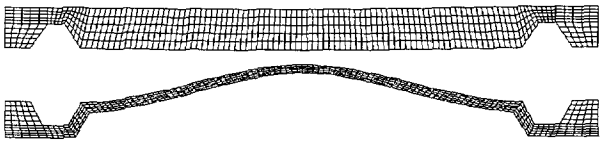

Fig. 5. — Mechanical deformations of the actuation unit of the micromechanical pump, when the electrodes are loaded by a voltage.

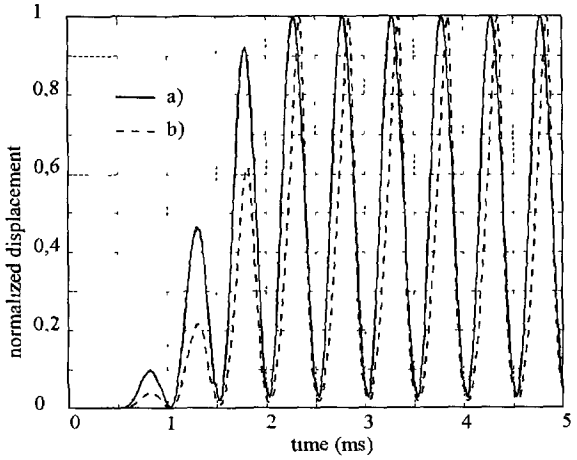

Fig. 6. — Mechanical displacement in the center of the pump diaphragm. a) Original amplitude of applied voltage. b) Twice the original amplitude of applied voltage.

behaviour was analyzed by computing the electrostatic-mechanical system with the described calculation scheme. In Figure 6, the center displacement of the elastic pump diaphragm is depicted as a function of the applied voltage The corresponding frequency spectra can be seen in Figure 7. For a good comparability each curve in Figures 6 and 7 is normalized to its maximum.

6.2. Acceleration Sensor. — In a second application example, a capacitive acceleration sensor, which is also fabricated by micromachined techniques was modeled. The Finite-Element / Boundary-Element model of this capacitive acceleration sensor is shown in Figure 8. The sensor consists of a fixed electrode 1, an etched silicon structure with counterelectrode 2 and a seismic mass. The size of the air gap between the electrodes is about 20 μm. Loading the sensor with an acceleration pulse causes the silicon structure to be deformed (Figure 9) and the change in the capacitance is a direct measure of the acceleration. Without using any controller, the silicon structure oscillates with its eigenfrequency to a new position according to the acceleration pulse (Fig. 10). Applying a PID-controlled voltage to the electrodes, the transient response can be kept to a minimum and the silicon structure moves to the old position (Fig. 10). Furthermore, the controller output (voltage, which is applied to the electrodes) is a direct measure of the acceleration.

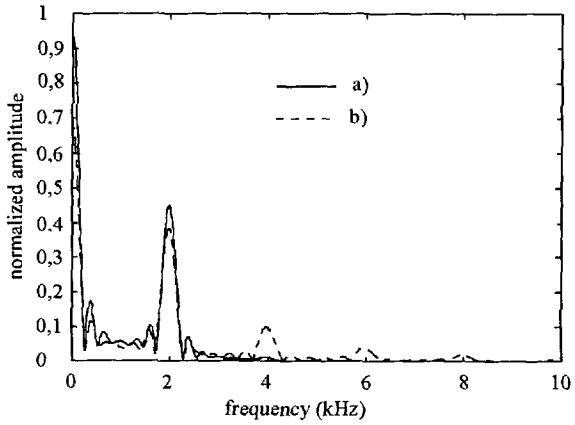

Fig. 7. — Frequency spectrum of the mechanical displacement in the center of the elastic pump diaphragm. a) Original amplitude of applied voltage. b) Twice the original amplitude of applied voltage.

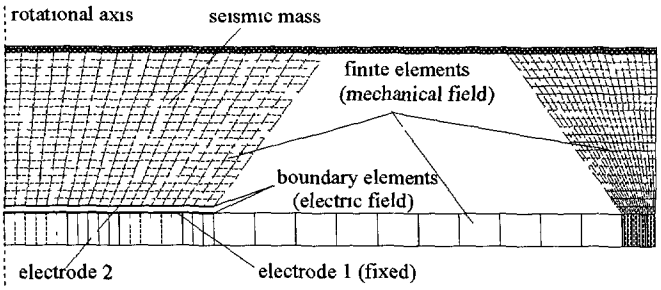

Fig. 8. — Finite Element - Boundary Element mesh of the acceleration sensor

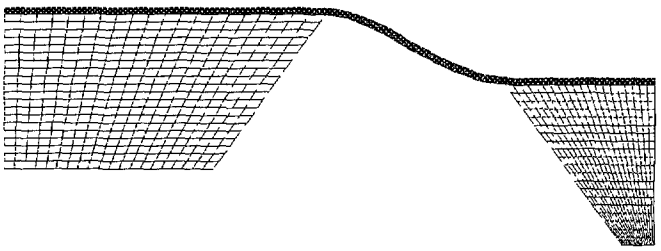

Fig. 9. — Deformations of the moving part of the acceleration sensor due to an acceleration pulse.

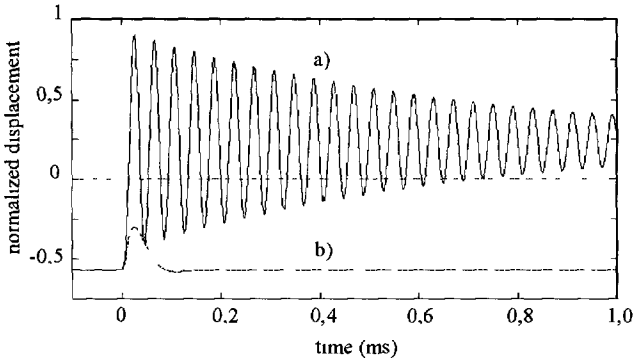

Fig. 10. — a) Uncontrolled dynamical behaviour due to an acceleration pulse. b) Controlled dynamical behaviour due to an acceleration pulse

7. Conclusion

A new approach for the numerical calculation of electrostatic-mechanical systems has been introduced. The use of the FEM-BEM coupling with a Predictor/Multicorrector algorithm, an efficient calculation scheme for the precise numerical computation of such systems has been achieved. Two practical examples (a micropump and an acceleration sensor) prove the applicability of the developed algorithm.

References

[1] Zengerle R., Kluge S., Richter M. and Richter A., A Bidirectional Silicon Mircopump, SENSOR 95, Nürnberg (1995) 727-732.
[2] Hughes T.J.R., The Finite Element Method, (New Jersey Prentice-Hall, 1987).
[3] Kaltenbacher M., Landes H. and Lerch R., A Strong Coupling Model for the Simulation of Magnetomechanical Systems using a Predictor/Multicorrector Algorithm, 7th International IGTE Symposium, Graz, 1996.